Die Angewandte Makromolekulare Chemie **213** *(1993) 127–155 (Nr. 3721)*

[1] Physical Chemistry II and
[2] Macromolecular Chemistry I, University of Bayreuth,
D-95440 Bayreuth, Germany
[3] Laser-Laboratorium Göttingen, D-37077 Göttingen, Germany

Dopant-induced laser ablation of PMMA at 308 nm: Influence of the molecular weight of PMMA and of the photochemical activity of added chromophores

Th. Lippert[1], A. Wokaun[1]*, J. Stebani[2], O. Nuyken[2]**, J. Ihlemann[3]

(Received 30 April 1993)

SUMMARY:

Polymers which are not absorbing at the wavelength of irradiation may be sensitized by doping with low concentrations of suitable compounds for laser-induced surface modification and ablation. In the present study this approach is applied to the ablation of PMMA by 308 nm irradiation (XeCl* excimer laser). Substituted phenyltriazene and diphenyltriazene compounds, two pentazadienes and a hexazadiene are tested as ablation promoters in concentrations of 1, 2, and 5 wt.-%, respectively. From all of these compounds, nitrogen is released upon photochemical decomposition.

A significant influence of the PMMA molecular weight on the ablation characteristics is found: higher molecular weights result in lower ablated depths per pulse. The etch rates achieved for the various dopants are correlated with the photophysical and photochemical parameters (i.e., absorption cross section and photolysis quantum yield) in solution. Above a characteristic minimum concentration of the additive, the ablated depth is approximately inversely proportional to the dopant concentration. In the regime of low laser fluence, the ablated depth per pulse scales with the logarithm of fluence, and is proportional to the quantum yield of photolysis in solution. For the limiting etch rate at high fluence, no correlation with the solution absorption cross section was found.

ZUSAMMENFASSUNG:

Polymere, die bei einer spezifischen Wellenlänge nicht absorbieren, können durch Dotierung mit geringen Konzentrationen geeigneter Verbindungen für die laserinduzierte Oberflächenmodifizierung und -ablation sensitiviert werden. In der vorliegenden Untersuchung fand diese Methode bei der Ablation von PMMA mit XeCl*-Excimer-

* Correspondence author.
** Present address: Institute of Technical Chemistry, Technical University of Munich, D-85748 Garching, Germany.

 CCC 0003-3146/93/$05.00

laserstrahlung von 308 nm Anwendung. Als Ablationspromotoren wurden mehrere substituierte Phenyl- und Diphenyltriazene, zwei Pentazadiene sowie eine Hexazadienverbindung in Konzentrationen von 1, 2 und 5 Gew.-% eingesetzt. Diese Substanzen setzen bei ihrer photochemischen Zersetzung Stickstoff frei. Das Ablationsverhalten des PMMA hängt von dessen Molekulargewicht in der Form ab, daß ein höheres Molekulargewicht zu geringeren Abtragtiefen pro Puls führt. Die mit den verschiedenen Promotoren erreichten Ätzraten sind mit deren photophysikalischen und photochemischen Eigenschaften in Lösung (z. B. dem Absorptionsquerschnitt und der Quantenausbeute bei der Photolyse) korreliert. Oberhalb einer charakteristischen Mindestkonzentration des Additivs verläuft die Abtragtiefe annähernd umgekehrt proportional zu dessen Konzentration. Im Bereich niedrigen Laserenergieflusses hängt die Abtragtiefe pro Puls logarithmisch vom Energiefluß ab und ist proportional zur Quantenausbeute bei der Photolyse in Lösung. Für die Grenzätzrate bei hohem Energiefluß wurde keine Korrelation zum Absorptionsquerschnitt in Lösung beobachtet.

Introduction

Since the early reports in 1982[1,2], the ablative photodecomposition of polymers became a field of intense investigation. For a survey on the general scope of the field, the reader is referred to recent reviews[3,4]. In this report we are focussing on the approach where polymers are doped with a small concentration of a chromophore, to achieve ablation at a wavelength where the pure polymer itself does not absorb. In such a case, no defined ablation (as contrasted with irregular surface damage) can be achieved without the addition of dopants.

Promising results on this route have recently been published for the ablation of PMMA by a 308 nm excimer laser, using diphenyltriazene (DPT)[5] or other chromophores[6,7] as dopants. This system is used as a reference point for the present study; the influence of the preparation technique of the polymer film on the ablation characteristics is investigated. The role of the molecular weight (M_w) of the polymer is examined, by using two defined PMMA samples with $M_w \approx 97000$ and 500000, respectively.

Hiraoka and co-workers[7] have stated that the photoetching rate and morphology after irradiation mainly depend on the polymer matrix, rather than on the dopant molecule. To test this hypothesis, and to obtain further insight into the mechanism of ablation, a series of differently substituted 1-aryl-3,3-dialkyltriazenes has been synthesized and dissolved in PMMA in concentrations of 1, 2, and 5 wt.-%. The ablation behaviour is correlated with the photophysical and photochemical parameters of the dopants in solution. The triazene compounds used differ in their photolysis quantum yields, which

span a wide range from 0.001 to 0.02. — In addition, two pentazadienes and one hexazadiene have been characterized and tested as ablation promoters in concentrations of 2 and 5 wt.-%.

Experimental

Instruments

Polymer samples were irradiated at 308 nm with a XeCl* excimer laser (Lambda Physik, model EMG 203 MSC). Pulses of ≈ 30 ns duration were delivered to the sample at a rate of 2 Hz, with the pulse energy adjusted by a variable attenuator (Laser-Laboratorium, Göttingen). The laser output was apertured by a 3.2 mm-diameter circular diaphragm, and imaged (9:1) onto the polymer surface by a 100 mm focal length lens. In this way, homogeneous illumination of a 375 μm-diameter circular area on the sample was achieved.

Materials

Structural formulas of the compounds used are shown in Scheme 1. The synthesis of 1-phenyl-3,3-dialkyltriazenes used for doping has been described in detail elsewhere[8]. The investigated compounds are identified in Tab. 1, where extinction coefficients and quantum yields of photolysis in solution are compiled.

Pentazadienes have been synthesized according to [9]. The hexazadiene synthesis was carried out as described in[10]; a detailed account will be given elsewhere.

PMMA of medium molecular weight (BDCh Chemicals, supplier's specification: M_w = 77500) was characterized by gel permeation chromatography resulting a molecular weight of 97000 ± 3000. A higher molecular weight PMMA sample (M_w = 500000) was obtained from Aldrich. For purification, the polymers were dissolved in tetrahydrofuran, and reprecipitated by dropping the solution into methanol.

Preparation of polymer films

PMMA was dissolved in tetrahydrofuran at a concentration of 5 wt.-%. 10–15 ml of the solution were poured into a glass dish of 4.5 cm in diameter, with a bottom plate of good planarity. The solvent was allowed to evaporate for 24 h. The film was then cut out of the dish, and vacuum-dried for 24 h. Final thickness corresponded to 200–300 μm.

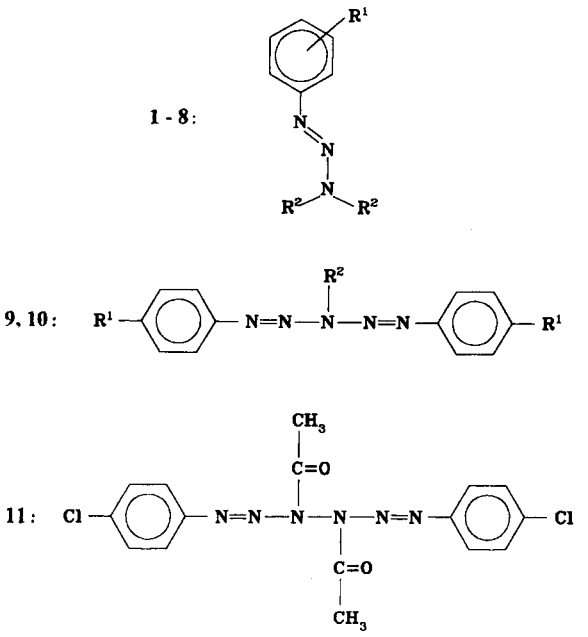

Scheme 1. Structural formulas of investigated triazenes (top), pentazadienes (middle), and hexazadiene (bottom). The substituents are identified in Tab. 1.

Results

Influence of the PMMA preparation technique

In the published reports[5] on the 308 nm ablation of PMMA doped with 1,3-diphenyltriazene (DPT), the appropriate amount of dopant was added into the neat liquid of methyl methacrylate monomer; radical polymerization was then started by the addition of AIBN. The resulting doped PMMA was cut into 1000–2000 μm thick discs, which were polished on both sides. As the triazene photolysis proceeds according to a radical mechanism in solution[11,12], it must be expected that the triazene dopant is attacked by the radicals during the polymerization and radical-induced decomposition cannot be excluded.

For this reason, it is of interest to compare the results of ref.[5] with the more gentle doping technique employed in the present study, in which PMMA of defined molecular weight (M_w = 97000) is dissolved in THF, and the solution

Tab. 1. Investigated Compounds for sensitizing PMMA ablation at 308 nm.

Label	Compound	Extinction coefficient ε at 308 nm (M^{-1} cm^{-1})	Quantum yield of photolysis in THF solution (%)
Substituted 1-phenyl-3,3-dialkyltriazenes (cf. Scheme 1, $R^2 = C_2H_5$): phenyl substituent R^1			
1	4-cyano	16900	0.36
2	3-nitro	16900	0.38
3	4-chloro	15800	0.40
4	4-nitro	5700	0.48
5	4-methyl	13800	0.60
6	4-methoxy	8000	1.33
7	4-dimethylamino	15900	10.6[a]
8	3-carboxy	10000	0.48
Substituted 1,5-diphenyl-3-alkylpentazadienes (cf. Scheme 1, $R^2 = C_2H_5$): phenyl substituent R^1			
9	4-chloro	12500	6.1
10	4-methyl	11200	11.6
Substituted 1,6-diphenyl-3,4-diacetylhexazadiene: phenyl substituent			
11	4-chloro	23600	5.7

[a] Quantum yield in methanol: 53%. Protolysis of 8 starts at pH 10.8; apparent yield of photolysis contains a contribution from acid-catalyzed decomposition.

is doped with the desired concentration of the DPT chromophore. Irradiation of the 200 μm thick cast PMMA films (cf. Experimental) was performed with the identical experimental setup that had been used in ref.[5].

Results are presented in Fig. 1 for DPT concentrations of 0.5, 1, and 2 wt.-%, respectively. The etch depths determined differ from those reported in ref.[5]. Refering to the limiting values of ablated depth per pulse at high fluence, we obtain an etch rate of 15 μm/pulse at the 2 wt.-% doping level, as compared to 10 μm/pulse in ref.[5]. For 1 wt.-% and 0.5 wt.-% doping, the data in Fig. 1 show etch rates of 25 and 40 μm/pulse, respectively, as compared to 15 and 30 μm/pulse[5].

Thus, the highest etch rate, 40 μm/pulse at 0.5 wt.-% doping, which was achieved for our cast polymer of molecular weight 97000, is higher by about 10 μm than had been observed for the PMMA discs[5]. For undoped reference samples, the observed ablation characteristics was equal for the two

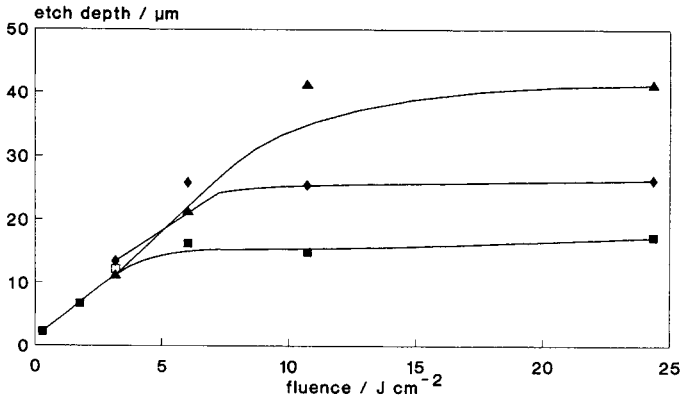

Fig. 1. Ablation of PMMA films ($M_w \approx 97000$) using a XeCl excimer laser at 308 nm. The ablated depth per pulse is determined as a function of laser fluence for a sample doped with 1,3-diphenyltriazene at concentrations of (▲) 0.5 wt.-%, (◆) 1 wt.-% and (■) 2 wt.-%, respectively.

preparation methods. Therefore, the different etch depth is not due to remaining solvent in the PMMA.

To elucidate the origin of these differences, some of the original PMMA samples employed in ref.[5] have been analysed by gel permeation chromatography (GPC). The results show an asymmetric distribution of molecular weights: a majority fraction of very long chains ($\overline{M}_w \approx 3 \cdot 10^6$) is accompanied by a broad distribution of lower molecular weights. In addition, evidence for modifications of the dopant during the radical polymerization has been obtained from the GPC experiments. With UV detection, the characteristic triazene absorption at 254 nm is found to be associated with the high M_w fractions of PMMA, which implies partial incorporation into the polymer. Some degradation products have also been detected. To further investigate the influence of the molecular weight distribution, two PMMA materials differing in their molecular weight will be compared in the next section.

Influence of the polymer molecular weight and of the dopant concentration

Results of ablation experiments performed on the two PMMA samples with defined molecular weight are presented in Fig. 2. The triazene (**1**) has been

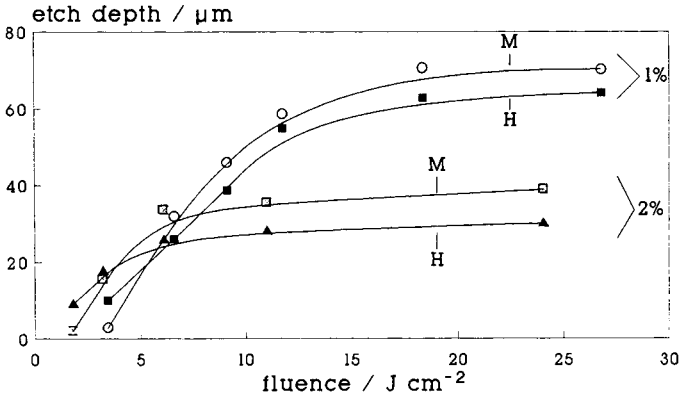

Fig. 2. Influence of the molecular weight on the ablation characteristics of PMMA doped with 1 and 2 wt.-% of 1-(4-cyanophenyl)-3,3-diethyltriazene (for structural formulas, refer to Scheme 1). The ablated depth per pulse is determined as a function of laser fluence for PMMA samples with medium ($M_w \approx 97000$, label M) and high ($M_w \approx 500000$, label H) molecular weights, as specified in the experimental section; (○) M/1 wt.-%, (■) H/1 wt.-%, (□) M/2 wt.-%, (▲) H/2 wt.-%.

used as the dopant at concentrations of 1 and 2 wt.-%, respectively (structural formula given in Scheme 1). Inspection of Fig. 2 shows that the dominant effect is due to the degree of doping; doubling the triazene concentration roughly halves the limiting etch depth per pulse. Within a given range of concentrations, this behaviour is in agreement with current theories of excimer laser-induced polymer ablation.

However, in addition a definite influence of the degree of polymerization is evident in Fig. 2. For the medium-molecular weight PMMA ($M_w \approx 97000$, denoted as 'M'), the high-fluence etch depths are higher by about 10% than the corresponding values obtained with the high-molecular weight PMMA ($M_w \approx 500000$, denoted as 'H' in Fig. 2).

This behaviour was confirmed for doping with the 1-(4-methoxyphenyl)-3,3-diethyltriazene monomer (**6**). At the 2 wt.-% doping level, the etch depth per pulse at high fluence amounts to about 50 µm/pulse for the high-M_w PMMA (H), and to ≈60 µm/pulse for the medium-M_w PMMA (M). We recall the analogous trend observed with DPT at the 2 wt.-% doping level: in ref.[5], the high-fluence etch depth was found to be 10 µm with a PMMA

sample of $M_w \approx 3 \cdot 10^6$, whereas in Fig. 1 we determined an etch depth of 15 μm with the $M_w = 97000$ sample M.

The maximum etch rate obtained with (**6**) for weaker doping at the 1 wt.-% level, is again higher, although not by a factor of 2 as had been observed with (**1**) (Fig. 2). For both triazene compounds, an upper limit of ablation of about 80 μm/pulse is reached at 1 wt.-% dopant concentration. To our knowledge, this is the highest ablation depth achieved on a synthetic polymer with a single pulse. The indicated value appears to represent an overall upper limit that can be reached with the present system, as will be discussed in more detail below.

Low dopant concentrations

For lower triazene concentrations (i.e., at 0.25 and 0.5 wt.-%) no defined ablation is achieved in the 0.5 – 20 $J \cdot cm^{-2}$ fluence range. However, a swelling of the irradiated areas of the polymer is revealed in the electron micrographs presented in Fig. 3. At low laser fluence (Fig. 3, top) an overall concave recession of the surface is observed. Small (≈ 1 μm in diameter) gas-filled bubbles apparently have been trapped underneath the surface. As the fluence is increased (middle micrograph), large convex bubbles are forming at the irradiated spots, which eventually explode at a fluence of 11.7 $J \cdot cm^{-2}$. The surface of each of these 400 μm-sized convex mounds is composed of smaller, 10 μm-sized bubbles filled with gaseous photoproducts, mainly nitrogen (see below).

Surface swelling has previously been observed at low fluences by Fukumura et al.[13]. The volume increase due to thermal depolymerization was found to lead to the development of complex mounds, with typical heights of a few μm, without the ejection of material. In our system, the mounds are higher (≈ 100 μm, cf. Fig. 3) and have the appearance of bubbles. As mentioned above, this shape is due to the photochemical decomposition reaction releasing nitrogen. Below the threshold for ablation, the nitrogen remains trapped in the polymer, giving rise to foam-like bubbles.

In order to remove the bulging-out material and to reveal a possible underlying crater, we attempted to use a mixture of methyl isobutyl ketone and isopropanol (3:1, v/v), which is a standard developer for PMMA electron beam resists[14]. This procedure which has been described for pure PMMA[15] was not successful in our case. Combined with other observations to be discussed below, this may be taken as an indication that a different mechanism of ablation is active in the present case.

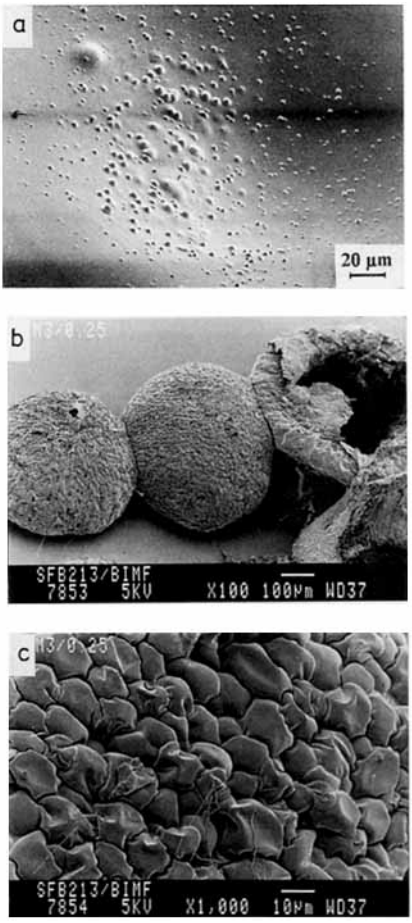

Fig. 3. Surface swelling and bubble formation at low dopant concentration. A medium-molecular-weight PMMA sample was doped with 0.25 wt.-% of triazene (**1**). Scanning electron micrographs were recorded after the following irradiations; a) single pulse of 0.79 J cm^{-2} fluence; b) single pulses with fluence increasing from left to right (3.5, 6.5, and 11.7 J cm^{-2}); c) surface of the bubble produced with 6.5 J cm^{-2} fluence imaged at a higher magnification.

Development of bubbles, rather than ablation, was also observed at the 1 and 2 wt.-% doping level at the lower limit of the fluence range, to be presented below in Fig. 4 and 5. This is the reason why, for several cases, the dependence of the etch depth d on laser fluence could not be followed down to $d \rightarrow 0$.

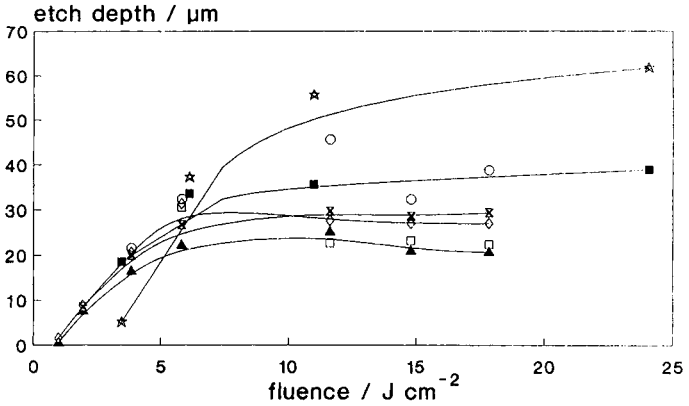

Fig. 4. Influence of the triazene dopant (**1**–**7**) on the 308 nm excimer laser ablation characteristics of PMMA films. The additives have been doped at a concentration of 2 wt.-% into a medium-molecular-weight PMMA sample ($M_w \approx$ 97000). The ablated depth per pulse is determined as a function of laser fluence. (■) **1**, (◇) **2**, (○) **3**, (⧖) **4**, (□) **5**, (☆) **6**, (▲) **7**.

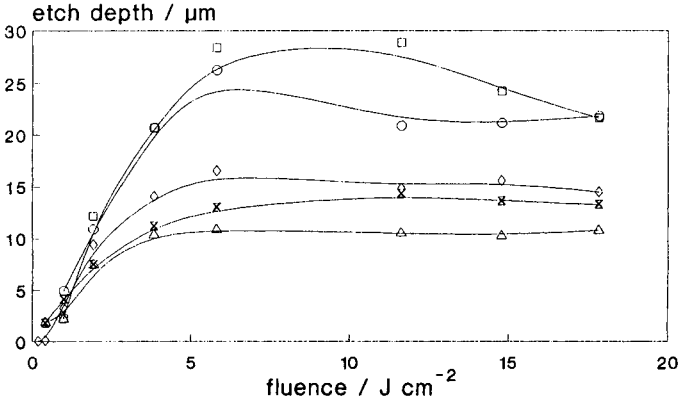

Fig. 5. Influence of the triazene dopant (**2**–**5**, **7**) on the 308 nm excimer laser ablation characteristics of PMMA films. The dopant concentration has been increased to 5 wt.-%; other parameters are the same as in Fig. 4.
(◇) **2**, (○) **3**, (⧖) **4**, (□) **5**, (▲) **7**.

Influence of the photochemical properties of the triazene additives

Whereas similar high-fluence etch rates are achieved for (**6**) and (**1**) at the 1 wt.-% concentration level, significant differences are observed for 2 wt.-% doping. A survey on the effect of seven differently substituted triazene additives on ablation in the lower-M_w PMMA sample is given in Fig. 4; the etch depth at high fluence is found to vary between ≈ 20 μm/pulse for the 4-methyl-(**5**), 4-dimethylamino-(**7**) and 3-carboxy-(**8**) 1-phenyl-3,3-diethyl-triazenes, and the highest value of ≈ 60 μm/pulse for the 4-methoxy derivative (**6**). Data for **8** are not shown in the figure.

The ablation characteristics for a higher dopant concentration of 5 wt.-% is presented for five triazene derivatives in Fig. 5. As expected from the previous subsection, the overall limiting etch rates are lower, varying between ≈ 10 and ≈ 25 μm/pulse.

Low-fluence and high-fluence regimes are apparent in the graphs of Fig. 4 or 5. However, an ordering of the dopants with respect to their efficiency for promoting the polymer ablation is not obvious; low- and high-fluence regimes will have to be discussed separately below.

An important parameter entering the discussion is the intrinsic quantum yield of photolysis in solution; we shall investigate whether the achieved etch rates parallel the photochemical activity. To this aim, solutions of the respective compounds in tetrahydrofuran (THF) have been irradiated with ≈ 140 mJ excimer laser pulses at 308 nm. Representative absorption curves taken from an extensive data set are presented in Fig. 6. From a quantitative analysis of the absorption decrease with the number of pulses delivered to the samples, photolysis quantum yields have been determined and are compiled in Tab. 1. Further details of these experiments in solution are described at another place[16].

The 4-dimethylamino derivative (**7**) represents an exceptional case. The apparent high quantum yield is, at least in part, due to protolysis (i.e., acid catalyzed decomposition of the compound) which proceeds in parallel with the photolysis. The 3-carboxy triazene (**8**) also exhibits a behaviour which is distinctly different from the fluence dependence observed with the other triazene derivatives. Although it is characterized by a high photolysis quantum yield in solution, the ablated depth per pulse is lowest among the three dopants investigated. An etch rate of ≈ 25 μm/pulse is observed at both concentrations of 1 and 2 wt.-%; remarkably, the ablated depth is more or less independent of laser fluence in the investigated range. No defined influence of the PMMA molecular weight is observed with this dopant either. Possible reasons for this unusual behaviour will be discussed below.

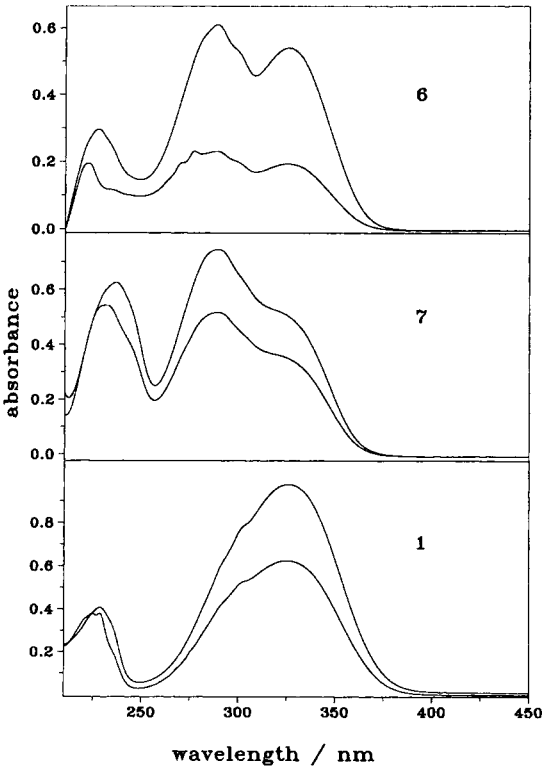

Fig. 6. Photolysis of triazene compounds **6**, **7**, and **1** in THF solution, at concentrations of $5.7 \cdot 10^{-5}$ M, $6.3 \cdot 10^{-5}$ M, and $4.9 \cdot 10^{-5}$ M, respectively. Absorption curves have been recorded before and after 50 excimer laser pulses at 308 nm ($\approx$ 140 mJ of energy) had been delivered to the sample.

Pentazadiene and hexazadiene dopants

Fluence-dependent etch rates achieved in PMMA (M_w = 97000) upon doping with 1,5-bis(4-chlorophenyl)-3-ethyl-pentazadiene (**9**), 1,5-bis(4-methoxyphenyl)-3-ethylpentazadiene (**10**), and 1,6-bis(4-chlorophenyl)-3,4-diacetylhexazadiene(1,5) (**11**) are presented in Fig. 7. Differences among these three dopants are not very pronounced. A clear concentration effect is again observed: With 2 wt.-% doping, high-fluence etch depths are in the range of $\approx$ 15 μm/pulse; at an additive concentration of 5 wt.-%, limiting etch rates vary between 7 and 9 μm/pulse. While these values are somewhat lower than

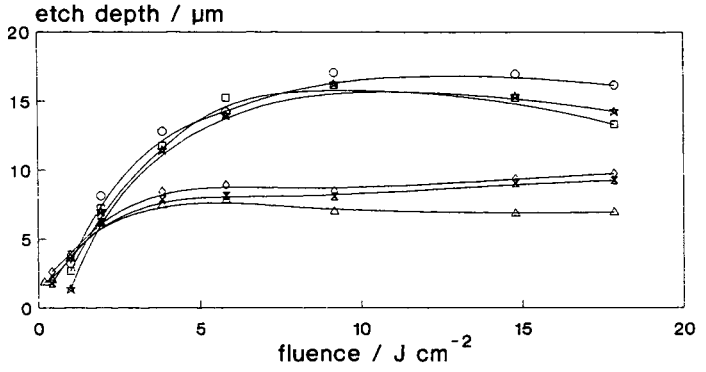

Fig. 7. Influence of pentazadiene and hexazadiene dopants on the 308 nm excimer laser ablation characteristics of PMMA films. The additives have been doped at concentrations of 2 and 5 wt.-% into an $M_w \approx 97000$ PMMA sample. (□) 2 wt.-% **9**, (△) 5 wt.-% **9**, (○) 2 wt.-% **10**, (◇) 5 wt.-% **10**, (☆) 2 wt.-% **11**, (⧖) 5 wt.-% **11**.

observed with the triazenes, the pentaza- and hexazadienes are attractive in view of the clean ablation craters achieved, as will be shown below.

Electron microscopy of crater profiles

Even in the absence of promoters, PMMA surfaces are modified with the use of very high excimer laser intensities. However, the necessary conditions do not give rise to satisfactory ablation profiles: exposure of undoped PMMA to high-fluence (≈ 10 J cm^{-2}) pulses just gives rise to brittle failure. In contrast, when 100 pulses of 1 J cm^{-2} fluence are delivered to PMMA doped with 5 wt.-% of triazenes **4** or **7**, deep conical holes in bulk plaques and via holes in 250 µm thick foils have been produced.

Focusing on the low fluence behaviour which is most important for microstructuring applications, the surfaces of six samples, each irradiated with 200 pulses of 0.2 J cm^{-2} fluence, are shown in Fig. 8. The dopant concentration was 5 wt.-% in each case. This fluence regime represents the transition from the surface swelling due to bubble formation, as described above, to the formation of clean ablation craters. This is best seen in the lower left micrograph, where the polymer has been removed from about half of the irradiated circular area, while a spongy mass resides on the other half. This

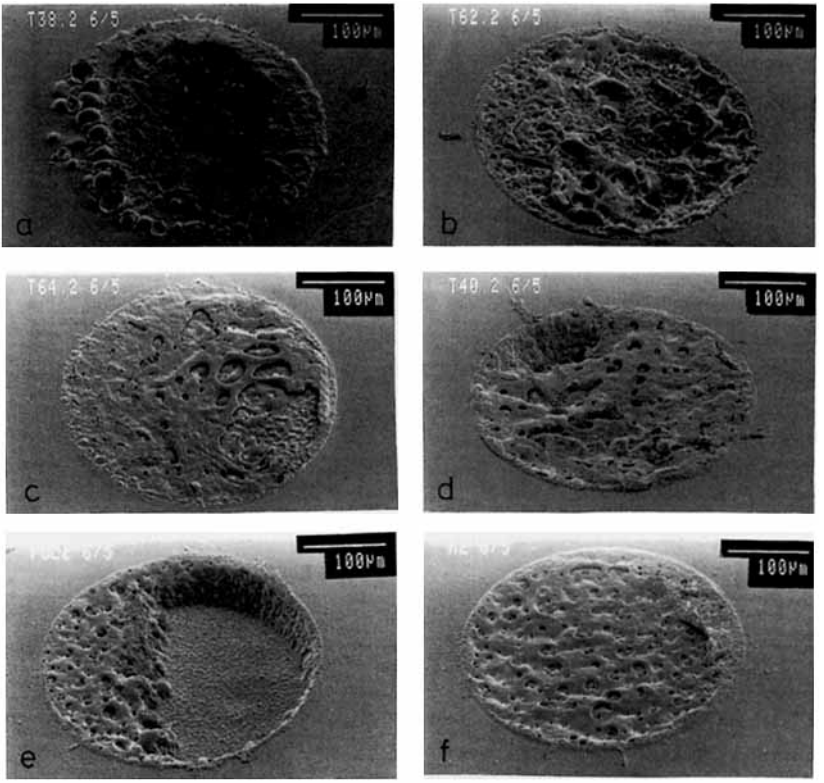

Fig. 8. Scanning electron micrographs of medium-M_w PMMA doped with 5 wt.-% of additives and irradiated with 200 pulses of 0.18 J cm^{-2} fluence. The following promoters have been used: a) **3**, b) **7**, c) **2**, d) **4**, e) **9**, f) **11**.

set of micrographs also illustrates why there is a lower limit of laser fluences where meaningful profilometer traces of the craters can be recorded. For this reason, the lowest laser fluences for which reliable etch depth data are available (Fig. 4 and 5) differs among the dopants investigated.

Although the conditions of Fig. 8 are certainly not useful for ablation, we note that the appearance of the irradiated surface already hints to the quality of the craters that can be produced when using higher fluences (Fig. 9). With dopant **3** (top left) a very rough surface with exploded bubbles and peeled-off areas is recorded. The surfaces appear somewhat more uniform for dopants **7** and **2**, but still there are ribbons and patches of molten and resolidified material. The micrographs of PMMA doped with triazene **4**, pentazadiene **9**

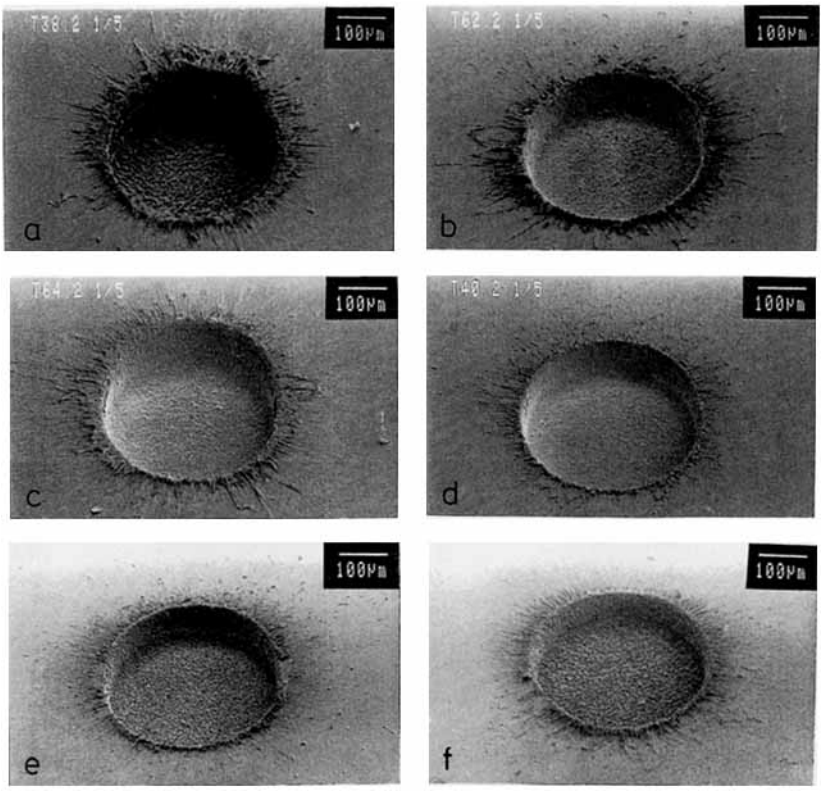

Fig. 9. Scanning electron micrographs of medium-M_w PMMA doped with 5 wt.-% of additives and irradiated with 5 pulses of 5.8 J cm^{-2} fluence. Promoters used are the same as in Fig. 8.

and hexazadiene **11** are comparable at this stage, showing a variety of holes through which photolytically produced nitrogen has escaped.

When the fluence per pulse at 308 nm is raised to 5.8 J cm^{-2}, well-defined ablation profiles result at the 5 wt.-% doping level. Representative micrographs recorded after 5 laser pulses are presented in Fig. 9. With dopant **3**, a large quantity of ejected material, partly in the form of polymer fibres, is seen around the edges of the crater. Both the walls and the bottom of the crater exhibit an irregular structure. Proceeding in the sequence from triazene **7** to the 3-nitro (**2**) and 4-nitro-derivatives (**4**), both the amount of ejected material and the roughness of the crater bottoms are reduced. The latter dopant, in particular, gives rise to steep and smooth crater edges. The investigated

pentazadiene **9** and hexazadiene **11** (bottom micrographs in Fig. 9) excel by rectangular profiles, even though the rim of ejected polymer is somewhat higher than observed with **4**.

The ablated depth per pulse is increased as the dopant concentration is reduced to 2 wt.-%, as mentioned above. The resulting consequences are illustrated in Fig. 10, where again each surface has been exposed to 5 pulses of 5.8 J cm^{-2} fluence. Generally, the deeper craters produced are rougher and less well-defined as compared to the analogous profiles described above for 5 wt.-% doping (Fig. 9). Triazene **3** again gives rise to the least satisfactory results, with a fibrous crater bottom and large amounts of ejected debris. As above, dopants **7** and **2** are comparable with regard to the appearance of the

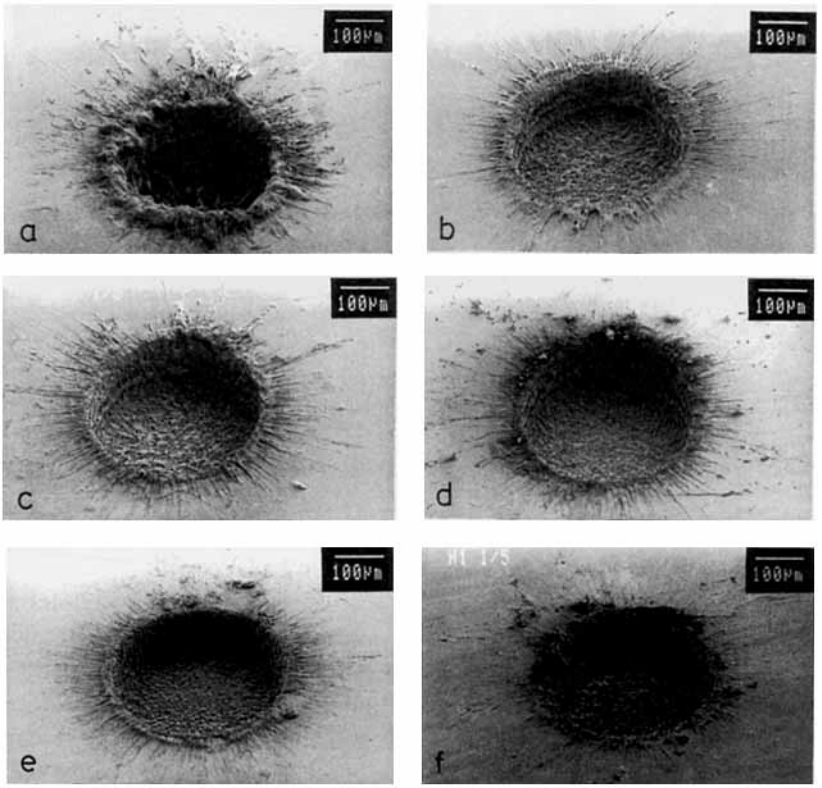

Fig. 10. Scanning electron micrographs of medium-M_w PMMA doped with 2 wt.-% of additives and irradiated with 5 pulses of 5.8 J cm^{-2} fluence. Promoters used are the same as in Fig. 8.

profiles. The most satisfactory results achieved with this series are recorded for the 4-nitrophenyl-diethyltriazene dopant (**4**), and for the pentazadiene **9**. The hexazadiene **11**, on the other hand, gives rise to a rough crater bottom and sloping walls under the present conditions.

Important details of both unsatisfactory and well-defined ablation craters are shown at higher magnification in the micrographs of Fig. 11. The fibrous structure of debris deposited around the crater edges when using the 4-dimethylamino-derivative (**7**) as a dopant is clearly visible in the top micrograph. The comparably rough crater bottom produced upon irradiation (at 5.8 J cm^{-2} fluence) of PMMA doped with 2 wt.-% of 1-(3-nitrohenyl)-3,3-diethyltriazene (**2**), exhibits holes and hillocks of resolidified material (middle micrograph). As the concentration for the same dopant is increased to 5 wt.-%, a much smoother crater bottom results (lower photograph).

The unusual fluence dependence observed with 1-(3-carboxyphenyl)-3,3-diethyltriazene (**8**) has been mentioned above. This dopant gives rise to ring-shaped walls of ejected material surrounding the circular crater which exhibits a rough and highly uneven bottom (not shown).

Very regular profiles (not shown) have also been recorded when using 1-(4-cyanophenyl)-3,3-diethyltriazene (**1**) as a dopant. While the appearance of the craters at lower fluences (2.75 J cm^{-2}) is comparable to the ones observed with triazenes **7** or **2**, an increase in fluence to 6.7 J cm^{-2} gives rise to defined circular craters. The totally ablated depth increases linearly with the number of pulses delivered. This is seen in some of the microraphs where the effects of successive pulses are discernible by rings of ejected material at the crater walls.

Analysis of the ejected material

At high fluences (>15 J cm^{-2}) fluffy material is ejected into the gas phase above the surface, which was collected and analysed by mass spectrometry. The material was found to be PMMA with a M_w higher than 2000. Similarly, the fibrous form of the deposits surrounding the crater walls (seen, e. g., in the electron micrograph of Fig. 11) suggests that the ejected debris mainly consists of PMMA. Analysis of the deposits on the PMMA surface by laser multiphoton ionization/mass spectrometry and vibrational spectroscopy is in progress.

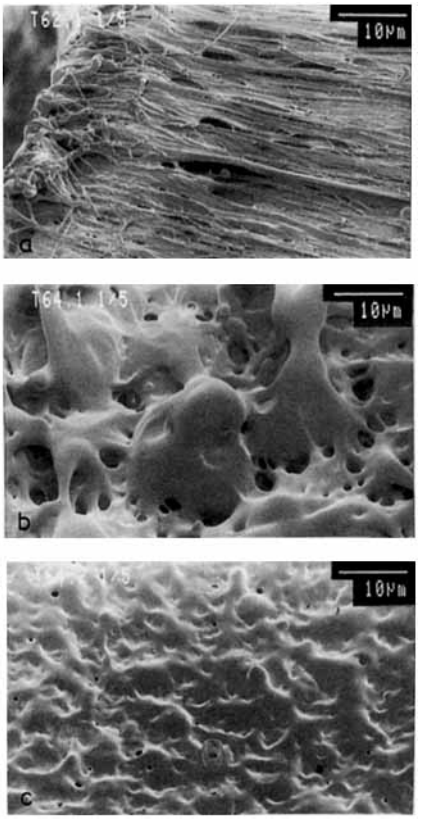

Fig. 11. Details of ablation craters at higher magnification: a) fibrous deposit around the ablation crater of PMMA doped with 2 wt.-% of 1-(4-dimethylaminophenyl)-3,3-diethyltriazene (**7**); b) crater bottom of sample doped with 2 wt.-% of 1-(3-nitrophenyl)-3,3-diethyltriazene (**2**); c) crater bottom of sample doped with 5 wt.-% of 1-(3-nitrophenyl)-3,3-diethyltriazene (**2**). In each case, the sample was irradiated with 5 pulses of 5.8 J cm^{-2} fluence.

Discussion

Influence of the polymer preparation method and molecular weight

The observed differences in the ablation behaviour of PMMA doped with 1,3-diphenyltriazene are addressed first. The optical quality was comparable for the two sets of samples. The cast PMMA foils were clear and transparent for 1 wt.-% doping, and coloured for dopant concentrations of 2 and 5 wt.-%,

resp. They have been irradiated as self-supporting films, with the beam entering from the side peeled off the glass dish, which exhibits a smoother surface quality. The plaques prepared by radical polymerization had been optically polished and appeared clear as well. The thickness of the samples (bulk plates vs. 200 μm cast films) might be of higher importance. Both the dissipation of heat by thermal conduction and the propagation of the shock wave associated with ablation are different for the two types of geometries.

The different ablation rates reported for the polymer samples prepared by radical polymerization in the presence of DPT on the one hand, and by dissolution of PMMA, physical doping with DPT, and film casting on the other hand, are mainly attributed to the simultaneous action of two mechanisms. Partial incorporation of DPT into the polymer backbone during the radical polymerization, accompanied by chemical modification, has been deduced from GPC analysis. These alterations are likely to reduce the tendency of the molecule to liberate nitrogen subsequent to absorption, i.e. the quantum yield of photolysis. On the other hand, the intrinsic absorption which determines the penetration depth appears to be largely unchanged. Taken together, these facts would lead to a lower ablated depth per pulse, as was indeed observed in ref.[5]. A crosslinking of PMMA chains induced by the presence of DPT would produce a polymer network that exhibits a higher resistance to ablation, and thus act in the same direction.

Another important parameter is, of course, the molecular weight and its distribution. For the two samples with different M_w investigated in this study, a definite influence of the molar mass has been demonstrated in Fig. 2. In the melt, the two PMMA samples differ in their viscosities. If the polymer melts upon irradiation before the eventual ejection of material[14], the lower viscosity of the low-M_w sample gives rise to the higher ablated depth. In addition, less energy per molecule is required at a smaller degree of polymerization. For the sample of ref.[5], an inhomogeneous distribution, with a main fraction of molar mass exceeding 10^6, has been determined. This fact is again consistent with the lower ablated depths per pulse found in ref.[5].

Mechanism of ablation

A few preliminary remarks concerning the mechanism of ablation can be made. Simple non-selective laser heating, i.e. thermal ablation[17], is of less importance for systems which do not exhibit ablation in the absence of dopants. For doped materials, both a 'photothermal'[7(b)] and a 'photo-

chemical'[6(b)] mechanism has been described. In the former case, energy is first selectively absorbed by the chromophore, and subsequently dissipated to the surrounding polymer by radiationless processes. The ablation itself would then proceed by a thermal mechanism, i.e. increase of the molar volume by melting and/or depolymerization. This model has been found to be important for the 308 nm ablation of PMMA doped with acridine[6(a)], benzophenone[7(c)], pyrene[7(a)], porphyrines[14], and the 'Tinuvin' stabilizer[6(b)]. However, all the quoted investigations have been working in a depth range of ≤ 10 μm ablated depth per pulse.

For triazene-doped systems, the photochemical mechanism appears to be of crucial importance, as may be judged from the much higher ablated depths per pulse. The nitrogen molecules released upon triazene photolysis are thought to act as the 'driving gas' for the ablation[5]. The dissociation of 1-aryl-3,3-dialkyltriazenes results, in addition, in the formation of several small molecules which could supplement the driving gas action of the nitrogen. In this respect, the aryl-dialkyltriazenes are different from DPT, where a reversible trans/cis isomerization competes with dissociation. This difference might account for the fact that the 1-aryl-3,3-dialkyltriazenes are more effective as dopants.

The production of 'driving gas' is a plausible explanation for the swelling of the polymer observed at low dopant concentrations and low laser fluences. In this case not enough nitrogen is produced to eject the material which is instead inflated into convex mounds.

The fact that we find the plateau values of the ablated depth per pulse to depend on the substitution pattern of the dopant, suggests that ablation mechanisms different from a simple thermally induced ejection are active in the present case. If just the deposition of energy in the polymer matrix was important, leading to zip depolymerization and hence an increase of the molar volume, one would expect the limiting depth to be independent of the quantum yield of photochemical decomposition. In the following sections, the dependence on the quantum yield will be tested both for the low- and the high-laser-fluence regimes.

Ablated depths per pulse in the low-fluence regime

When discussing the ablated depth per pulse, various fluence ranges must be distinguished. For the example of DPT, the fluence dependence is presented on a logarithmic scale in Fig. 12 (these data have earlier been presented on a linear fluence scale[5]). A 'linear' regime[3] in which the etch rate increases with

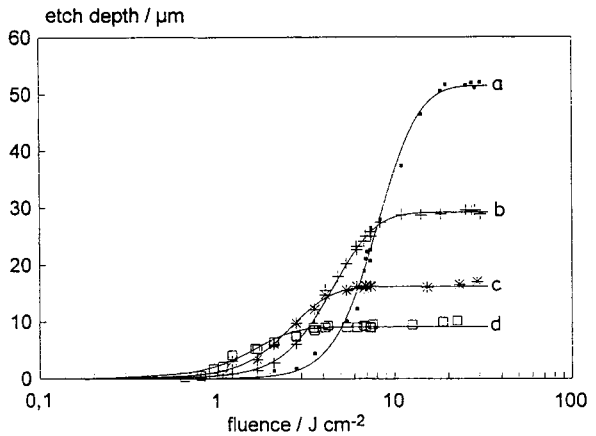

Fig. 12. Dependence of the ablated depth per pulse on the logarithm of laser fluence at 308 nm, for PMMA doped with (a) 0.25, (b) 0.5, (c) 1 and (d) 2 wt.-% of 1,3-diphenyltriazene.

the logarithm of fluence, as found also in the ablation of absorbing undoped polymers[4], is followed by a plateau region in which the ablated depth becomes approximately independent of fluence.

The linear range is addressed first. The layer thickness that can be ablated per pulse is determined by two counteracting effects. The lower the dopant concentration, the higher is the penetration depth, thereby inducing photodegradation in a thicker layer (Fig. 2). On the other hand, the number of nitrogen molecules produced and the energy transferred to the polymer per unit volume both are decreasing with the concentration. If the specific production of driving gas remains below a minimum value, no ablation is observed.

The role of photolysis quantum yield QY < 1 may be discussed in terms of this model. Part of the absorbed photon energy is dissipated into other channels, in which no nitrogen is produced. This 'additional absorption' reduces the penetration without increasing the driving gas production. One would therefore predict that the ablatable depth per pulse should scale with the photolysis quantum yield, provided that gas production is the important mechanism for ablation. In the linear range, one would then obtain for the depth d(F), ablated at a given laser fluence F, a relation of the form

$$d(F) \propto \frac{QY}{\sigma \cdot c_{dopant}} \ln (F/F_0) \qquad \text{for } c_{dopant} \geq c_{min} \tag{1}$$

In this equation, σ [cm^2] is the absorption cross section, c_{dopant} [cm^{-3}] is the volume concentration of dopant molecules, and F_0 represents a threshold fluence to be discussed below.

Unfortunately, the parameters introduced in Eq. 1 are interdependent. As the minimum dopant concentration c_{min} is related to nitrogen production, this parameter is expected to be inversely proportional to the quantum yield QY. Furthermore, for doped systems the threshold fluence F_0 is a formal parameter that depends on dopant concentration. The determination of F_0 from a plot of ablated depths per pulse, d, against the logarithm of laser fluence is illustrated in Fig. 12 for PMMA doped with DPT. For a given dopant concentration, F_0 is obtained from the abscissa intercept of the linear part of the etch rate curve, extrapolated to $d \rightarrow 0$. We note that the higher c_{dopant}, the lower is the minimum laser fluence required to produce a sufficient quantity of driving gas per volume. Thus, for a given polymer/

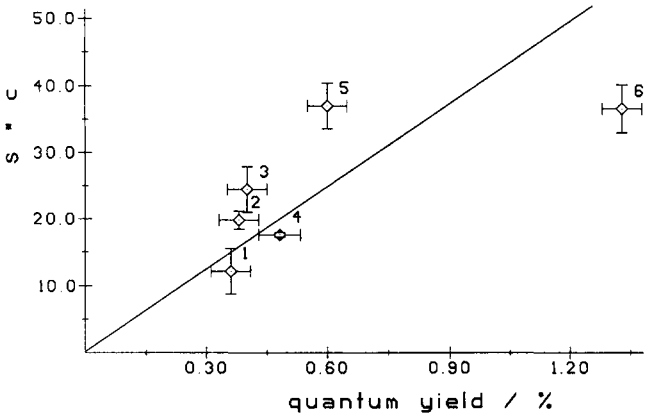

Fig. 13. Dependence of the etch rate on the quantum yield of photolysis in solution for the low-fluence regime. From a plot of the ablated depth per pulse, d, against ln (F/mJ cm^{-2}) according to Eq. 1, the slope s was evaluated. In this figure, the quantity ($s \cdot c_{dopant}$/wt.-%) is graphed against the photolysis quantum yield in solution. Triazene additives were identified by symbols according to Tab. 1.

dopant system, F_0 is not a constant but decreases with the concentration of the additive. In fact, for PMMA/diphenyltriazene, the intercept fluence in Fig. 12 is seen to scale as $1/c_{dopant}$ in the concentration range from 0.25 to 1 wt.-%. As a consequence of the variation in F_0, the curves characterizing the etch rate as a function of fluence for various concentrations are crossing,

and the ablated depth per pulse may be higher for heavily doped materials at low laser fluence.

To test the validity of the proposed relationship, Eq. (1), the low-fluence etch rates have been graphed against the logarithm of fluence for all of the investigated triazene dopants. Linear regression yields both the threshold fluence F_0, and the slope s, which according to Eq. 1 should be proportional to $[QY/(\sigma \cdot c_{dopant})]$. The values obtained from the least squares analysis are included in Tab. 2. In Fig. 13, the quantities $(s \cdot c_{dopant})$ are plotted against the corresponding photolysis quantum yield of the dopant in solution, as reported in Tab. 1. A satisfactorily linear dependence with a correlation coefficient of 0.70 is obtained. Most remarkably, the intercept of the regression line is zero within the confidence limits, as required by Eq. 1. With compound **7**, decomposition proceeds by concurrent photolysis and fast acid-catalyzed degradation, as mentioned above. For triazene **8**, we have indicated that no regular dependence of etch depth on the fluence was observed. These two substances have therefore not been included in the present analysis.

As the correlation obtained in Fig. 13 is only fair, it appeared necessary to test whether the data would also be compatible with a thermal mechanism of

Tab. 2. Ablation parameters of PMMA doped with the investigated compounds.

	Threshold fluence F_0 (J cm^{-2})		Low-fluence slope s (μm)[a]		High-fluence $d_{plateau}$ (μm)[b]	
Compound label	Concentration in wt.-%					
	2	5	2	5	2	5
1	1.74	—	26.2	—	40	—
2	1.00	0.47	16.5	6.5	28	17
3	1.34	0.71	21.4	12.2	≈40	25
4	1.13	0.31	16.4	4.4	30	13
5	—	0.85	—	14.3	≈30	28
6	2.92	—	43.6	—	60	—
7	1.01	0.33	12.3	4.1	23	11
8					21	
9	0.68	0.10	7.0	2.0	15	7
10	0.52	0.17	6.1	2.6	17	8
11	0.67	0.22	6.1	2.8	16	8

[a] From a fit of low-fluence etch rates versus ln (F/mJ cm^{-2}) according to Eq. 1.
[b] Maximum ablated depth per pulse at high fluence.

ablation. For the latter, an accepted criterion[13] is that the threshold fluence F_0 should be related to the minimum temperature rise required to drive the ablation process. When comparing related systems for different dopants or dopant concentrations, the quantity F_0/s should be constant[13], where s is the slope in a plot of the etch rate against ln F, as in Eq. 1. We have tested this relationship and find that F_0/s is indeed approximately constant within the (comparatively large) error bars. The associated temperature rise corresponds to about 350–400 K.

In summary, the ablated depth per pulse depends linearly on the logarithm of fluence in the range below a few J cm^{-2}. The slope of this dependence on ln (F/F_0) is inversely proportional to the dopant concentration and proportional to the quantum yield of photolysis in solution. The latter conclusion, derived from Fig. 13, strongly suggests an important contribution of the photochemical ablation mechanism in the low-fluence regime. This finding justifies our approach to improve the ablation characteristics by enhancing the photophysical properties of the dopant molecule. In view of the comparatively large scatter in the data, a significant contribution of the thermal ablation mechanism cannot be ruled out as well.

The 1-(3-carboxyphenyl)-3,3-diethyltriazene compound (**8**) represents a remarkable exception. The photolysis quantum yield of the substance in solution is higher than the one of **1**, i.e. 0.48% in THF (cf. Fig. 5) and 1.6% in methanol. Yet, the ablation efficiency of this dopant is poor, as judged from the lower depths per pulse recorded and their relative intensitivity to laser fluence. Compound **8** contains a carboxylic acid group which might be involved in hydrogen bridges to polar groups of the PMMA, thereby reducing the ablation depth. Furthermore, the —COOH groups can may be split off by decarboxylation, as has been established by differential scanning calorimetry and thermal gravimetric analysis[8]. Protons liberated in this process would tend to destroy further triazene dopant molecules which are quite unstable in acids[18]. In this context, the fast protolytic decomposition of **7** is recalled.

Limiting etch rate at high laser fluence

The results obtained with triazene dopants indicate that, for the lowest useful dopant concentrations of $\approx$ 1 wt.-%, the ablated depth does not exceed a maximum value of ≈ 80 μm/pulse. Recent investigations on the pulsed laser ablation of human cornea tissue[19] are helpful for interpreting the observed behaviour. Upon doping of cornea tissue with fluorescein and irradiation at 485 nm, an ablation depth of ≈ 80 μm was reported[19] and found to be

independent of fluence in the 10–100 J cm^{-2} range. With oxy-buprocaine doping and 308 nm irradiation, a plateau value in the ablated depth of ≈ 33 μm was reached at a fluence of 7 J cm^{-2}. The water content of the tissue was found to have a pronounced influence on the ablated depth; for this system the gaseous water formed would again act as a driving gas.

Several authors have drawn attention to the non-uniform dependence of the ablated depth on fluence, which may involve one or two plateau values[19]. Absorption and scattering by the ablated material in the plume[20,21], as well as transmittance increase due to the saturation of absorption at higher fluences[21], have been discussed. At even higher power densities, laser-induced plasma creation gives rise to avalanche-type effects, plasma absorption and increased surface reflectivity[22].

The present data provide experimental evidence that the plateau etch depth $d_{plateau}$ is approximately proportional to the inverse dopant concentration (Fig. 2, 4, 5, and 7). It is of interest to test whether $d_{plateau}$ scales with a (positive or negative) power of the absorption cross section σ. A plot of the limiting etch rates against the molar absorption coefficients at 308 nm (Tab. 1) is presented in Fig. 14, for dopant concentrations of 2 and 5 wt.-%, respectively.

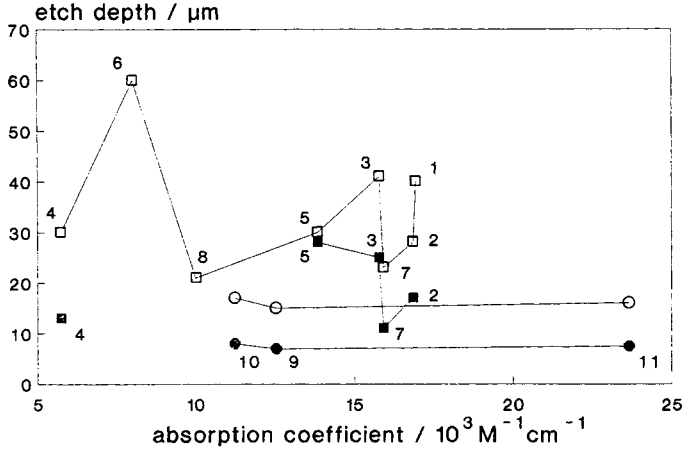

Fig. 14. Limiting etch depth per pulse, $d_{plateau}$, for triazenes {(□) compounds **1** to **8**}; pentazadienes {(○) compounds **9** and **10**} and the hexazadiene **11** (○). Open and full symbols denote dopant concentrations of 2 and 5 wt.-%, respectively. The graph shows that $d_{plateau}$ does not exhibit an obvious correlation with the absorption coefficient σ at 308 nm in solution (abscissa). Solid lines are just guides to the eye.

A decrease in the plateau etch rate by a factor of 2.5 is expected as the dopant concentration is increased from 2 to 5 wt.-%. For the pentazadiene and hexazadiene additives, this relation is well fulfilled. With the triazenes, the plateau etch depths are also consistently lower for the more heavily doped samples, although not always by a full factor of 2.5. (We note that no data for 5 wt.-% doping are available for the 1-(4-cyanophenyl)- and 1-(4-methoxyphenyl)-3,3-diethyltriazene derivatives **1** and **6**, respectively. Solid lines in Fig. 14 are just guides to the eye by connecting the data sets corresponding to different concentrations). — At this point, one should emphasize that the relationship $d_{plateau} \propto c_{dopant}^{-1}$ is an approximate one. For example, with PMMA/diphenyltriazene (Fig. 12), the limiting etch rate is increased by a factor of 1.8 as the dopant concentration is reduced by a factor of 2; with other systems the corresponding increase is somewhat smaller.

From Fig. 14 $d_{plateau}$ appears to be independent from the absorption cross section for the pentazadienes and the hexazadiene. With the triazene dopants there is at least no obvious simple dependence on σ alone.

The lack of a correlation between $d_{plateau}$ and σ could, of course, be due to the fact that other parameters, such as the quantum yield, are important as well. To test for this possibility, several other reasonable combinations of experimental quantities have been graphed against each other, and were tested for a correlation. For example, the quantities $(d_{plateau} \cdot \sigma)$ and $(d_{plateau} \cdot \sigma \cdot c_{dopant})$ were plotted against the quantum yield of photolysis in solution. For both cases, the data exhibit large scatter, and no correlation was indicated by linear regression analysis.

A simple estimate shows that at the onset of saturation, the number of absorbed photons is typically ≈ 100 times higher than the number of dopant molecules in the ablated volume. Thus, mainly the absorption of energy by dopant molecules, reaction intermediates and photolysis products will be of importance. At this stage, a thermal mechanism, i.e. the absorption of photons followed by thermalization of the energy, provides the dominant contribution to the ablation. Therefore, the photolysis quantum yield QY appears to be no longer of importance.

The lack of a correlation with the absorption cross section σ is more astonishing. However, the quantity governing the energy deposition per volume during the process of ablation is not just the linear absorption cross section of the reactant, but the weighted average of the corresponding absorptivities of all relevant species present during the photolysis under high-fluence conditions. The characterization of photolysis intermediates and their reactivities in the respective excited states will require extensive further experimentation.

Conclusions

The results presented in this study demonstrate that non-absorbing polymers can be efficiently doped for 308 nm excimer laser ablation, by adding small concentrations of substituted 1-phenyl-3,3-dialkyltriazene derivatives. Crater formation is induced by a photochemical ablation mechanism based on the photolytic fragmentation of the dopant. Nitrogen acts as a driving gas for the ejection of polymer material. Ablated depths per pulse as high as 80 μm have been observed with the compounds 1-(4-cyanophenyl)-(**1**) and 1-(4-methoxyphenyl)-3,3-diethyltriazene (**6**), as described in the text.

Scanning electron micrographs of the ablation craters and an analysis of the etch rates reveal that even within a class of structurally similar promoters, the electronic and photophysical parameters of the dopant molecule have a pronounced influence on the ablation behaviour.

The data also show that much care is required in the quantification of polymer ablation experiments. The source of the polymer[23], the molecular weight, the shape of the corresponding distribution of molar masses and the preparation of the samples all have a potential influence on the laser etching rates.

The dependence of the etch rate on laser fluence exhibits two regimes, i.e. a linear dependence on the logarithm of fluence $\{\ln (F/F_0)\}$ followed by a plateau region. In the linear regime, the ablated depth per pulse is proportional to the quantum yield of photochemical decomposition, and follows the $1/c$ dependence known from other studies of both doped and undoped polymers.

According to the limited data set available, the plateau etch rate for the high-fluence regime is found to scale with $(c_{dopant})^{-1}$, i.e. it is again inversely proportional to the dopant concentration. No clear dependence on the solution absorption cross section of the promoter at the laser wavelength, nor on the quantum yield of photolysis in solution, has been identified. However, a pronounced dependence on the specific substitution pattern is apparent even within the investigated series of structurally similar triazene derivatives. This information is important in view of the earlier suggestion that the nature of dopants was of less importance as compared to the properties of the polymer to be ablated.

For a given chromophore, the maximum etch rate is achieved at a defined minimum dopant concentration c^*_{min}, which is required for sufficient energy deposition. One would expect that the lower the absorption coefficient, the higher is c^*_{min} for systems with comparable photophysical characteristics.

More extensive series of dopant concentrations are required to elucidate this dependence.

Physical doping of non-absorbing polymers with low concentrations of chromophores may be compared with an alternative approach where the absorbing group (here, the triazene functionality) is covalently bound to the polymer, either as a side chain or in the backbone. The use of triazene polymers is attractive, as well-defined craters with sharp edges and flat bottoms may be formed[24]. However, the ablated depths per pulse achieved with this complementary technique are typically smaller by an order of magnitude, as compared with the results obtained in the present system.

We are indebted to F. Zimmermann for his valuable assistance. Financial support of this work by grants of the Deutsche Forschungsgemeinschaft (SFB 213), by the Verband der Chemischen Industrie und by the BMFT (project 13N 5621-5) is gratefully acknowledged.

[1] Y. Kawamura, K. Toyoda, S. Namba, Appl. Phys. Lett. **40** (1982) 374
[2] R. Srinivasan, V. Mayne-Banton, Appl. Phys. Lett. **41** (1982) 576
[3] S. Lazare, V. Granier, Laser Chem. **10** (1989) 25
[4] R. Srinivasan, B. Braren, Chem. Rev. **89** (1989) 1303
[5] (a) M. Bolle, K. Luther, J. Troe, J. Ihlemann, H. Gerhardt, Appl. Surf. Sci. **46** (1990) 279
(b) J. Ihlemann, M. Bolle, K. Luther, J. Troe, Proc. SPIE-Int. Soc. Opt. Eng. **1361** (1991) 1011
[6] (a) R. Srinivasan, B. Braren, R. W. Dreyfus, L. Hadel, D. E. Seeger, J. Opt. Soc. Am. **B 3** (1986) 785
(b) R. Srinivasan, B. Braren, Appl. Phys. A: **A45** (1988) 289
[7] (a) H. Hiraoka, T. J. Chuang, H. Masuhara, J. Vac. Sci. Technol. **B 6** (1988) 463
(b) T. J. Chuang, H. Hiraoka, A. Mödl, Appl. Phys. A: **A45** (1988) 277
(c) H. Masuhara, H. Hiraoka, K. Domen, Macromolecules **20** (1987) 450
[8] J. Dauth, Th. Lippert, O. Nuyken, A. Wokaun, Magnet. Res. Chem. **30** (1992) 1178
[9] M. Remes, J. Divis, V. Zverina, M. Matrka, Chem. Prum. **23** (1973) 133
[10] D. Mackay, D. D. McIntyre, N. J. Taylor, J. Org. Chem. **47** (1982) 532
[11] J. Baro, D. Dudek, K. Luther, J. Troe, Ber. Bunsen-Ges. Phys. Chem. **87** (1983) 1155
[12] J. Baro, D. Dudek, K. Luther, J. Troe, Ber. Bunsen-Ges. Phys. Chem. **87** (1983) 1161
[13] H. Fukumura, N. Mitsuka, S. Eura, H. Masuhara, Appl. Phys. A: **A53** (1991) 255
[14] G. H. Bernstein, D. Hill, W.-P. Liu, J. Appl. Phys. **71** (1992) 4066
[15] R. Srinivasan, B. Braren, K. G. Casey, J. Appl. Phys. **68** (1990) 1842

[16] (a) Th. Lippert, B. Metzner, D. Franzke, J. Dauth, J. Stebani, O. Nuyken, A. Wokaun, 14th IUPAC Conference, Leuven, July 1992;
(b) J. C. Panitz, Th. Lippert, J. Stebani, O. Nuyken, A. Wokaun, J. Phys. Chem. **97** (1993) 5246;
(c) Th. Lippert, J. Stebani, O. Nuyken, A. Stasko, A. Wokaun, J. Photochem. Photobiol. A (1993), in press

[17] D. Dijkkamp, A. S. Gozdz, T. Venkatesan, X. D. Wu, Phys. Rev. Lett. **58** (1987) 2142

[18] D. M. Julliard, C. J. Michejeda, J. Am. Chem. Soc. **442** (1981) 103

[19] W. Husinsky, S. Mitterer, G. Grabner, J. Baumgartner, Appl. Phys. B: **49** (1989) 463

[20] G. M. Davis, M. C. Gower, J. Appl. Phys. **61** (1987) 2090

[21] G. H. Pettit, R. Sauerbrey, Appl. Phys. Lett. **58** (1991) 793

[22] F. Cornolti, P. Mulser, M. Hahn, in: Lasers and Particle Beams, Cambridge University Press, Cambridge 1991, Vol. 9, p. 465

[23] P. P. van Saarloos, J. J. Constable, J. Appl. Phys. **68** (1990) 377

[24] Th. Lippert, A. Wokaun, J. Stebani, O. Nuyken, J. Ihlemann, Angew. Makromol. Chem. **206** (1993) 97